

**1 Transpiration from subarctic deciduous woodlands: environmental controls and  
2 contribution to ecosystem evapotranspiration.**

3 Ana M. Sabater <sup>1,2,3,4</sup>, Helen C. Ward <sup>5</sup>, Timothy C. Hill <sup>6</sup>, Jemma L. Gornall<sup>7</sup>, Thomas  
4 J. Wade <sup>8</sup>, Jonathan G. Evans <sup>9</sup>, Ana Prieto-Blanco <sup>10</sup>, Mathias Disney <sup>10, 11</sup>, Gareth K.  
5 Phoenix <sup>12</sup>, Mathew Williams <sup>8</sup>, Brian Huntley <sup>13</sup>, Robert Baxter <sup>13</sup>, Maurizio  
6 Mencuccini <sup>2, 14</sup>, Rafael Poyatos <sup>1, 2, 15</sup>

7

8 <sup>1</sup> Universitat Autònoma de Barcelona, Barcelona, Spain.

9 <sup>2</sup> CREAM, Cerdanyola del Vallès, Barcelona, Spain.

10 <sup>3</sup> Fundación CEAM, Joint Research Unit University of Alicante-CEAM, Alicante,  
11 Spain.

12 <sup>4</sup> Department of Ecology, University of Alicante, Alicante, Spain.

13 <sup>5</sup> Department of Atmospheric and Cryospheric Sciences (ACINN), University of  
14 Innsbruck, Innsbruck, Austria.

15 <sup>6</sup> College of Life and Environmental Sciences, Department of Geography, University of  
16 Exeter, Exeter, UK.

17 <sup>7</sup> Met Office, Exeter, UK.

18 <sup>8</sup> School of Geosciences, University of Edinburgh, Edinburgh, UK.

19 <sup>9</sup> Centre for Ecology and Hydrology, Wallingford, UK.

20 <sup>10</sup> University College London, Department of Geography, London, UK.

21 <sup>11</sup> NERC National Centre for Earth Observation (NCEO), Leicester, UK.

22 <sup>12</sup> Department of Animal and Plant Sciences, University of Sheffield, Sheffield, UK.

23 <sup>13</sup> Department of Biosciences, Durham University, Durham, UK.

24 <sup>14</sup> ICREA, Barcelona, Spain.

25 <sup>15</sup> Laboratory of Plant Ecology, Faculty of Bioscience Engineering, Ghent University,  
26 Ghent, Belgium.

27 Correspondence. R. Poyatos, CREAM, Edifici C, Campus UAB Bellaterra, E08193  
28 Barcelona, Spain. Email: [r.poyatos@creaf.uab.es](mailto:r.poyatos@creaf.uab.es), Tel.+34 935814676, Fax:  
29 +34935814151.

30 Short title: Transpiration and evapotranspiration of subarctic deciduous woodlands

## 31 **Abstract**

32 Potential land-climate feedbacks in subarctic regions, where rapid warming is driving  
33 forest expansion into the tundra, may be mediated by differences in transpiration of  
34 different plant functional types. Here we assess the environmental controls of overstorey  
35 transpiration and its relevance for ecosystem evapotranspiration in subarctic deciduous  
36 woodlands. We measured overstorey transpiration of mountain birch canopies and  
37 ecosystem evapotranspiration in two locations in northern Fennoscandia, having dense  
38 (Abisko) and sparse (Kevo) overstories. For Kevo, we also upscale chamber-measured  
39 understorey evapotranspiration from shrubs and lichen using a detailed land cover map.  
40 Sub-daily evaporative fluxes were not affected by soil moisture, and showed similar  
41 controls by vapour pressure deficit and radiation across sites. At the daily timescale,  
42 increases in evaporative demand led to proportionally higher contributions of overstorey  
43 transpiration to ecosystem evapotranspiration. For the entire growing season, the  
44 overstorey transpired 33% of ecosystem evapotranspiration in Abisko and only 16% in  
45 Kevo. At this latter site, the understorey had a higher leaf area index and contributed  
46 more to ecosystem evapotranspiration compared to the overstorey birch canopy. In  
47 Abisko, growing season evapotranspiration was 27% higher than precipitation,  
48 consistent with a gradual soil moisture depletion over the summer. Our results show that  
49 overstorey canopy transpiration in subarctic deciduous woodlands is not the dominant  
50 evaporative flux. However, given the observed environmental sensitivity of  
51 evapotranspiration components, the role of deciduous trees in driving ecosystem  
52 evapotranspiration may increase with the predicted increases in tree cover and  
53 evaporative demand across subarctic regions.

## 54 **Keywords**

55 Arctic, branch cuvettes, eddy covariance, evapotranspiration partitioning, mountain  
56 birch, tundra, understorey

57

## 58 Introduction

59 Northern high latitudes (boreal and arctic biomes) exert an important influence in global  
60 biosphere-atmosphere interactions involving water, energy and atmospheric  
61 composition. These interactions are globally relevant because of the large extent of  
62 these biomes (arctic tundra and boreal forest cover *ca.*  $1.24 \cdot 10^8$  km<sup>2</sup>) and the intense  
63 and rapid warming occurring at northern high latitudes (0.5 K/decade since 1979; IPCC,  
64 2013), which is partly driven by regional positive feedbacks (Chapin et al., 2000).  
65 Warmer temperatures and longer growing seasons are already inducing poleward and  
66 altitudinal treeline migration and shrub expansion in the tundra zone, which may in turn  
67 drive considerable land-atmosphere feedbacks in these latitudes (Kattsov et al., 2005;  
68 Swann, Fung, Levis, Bonan, & Doney, 2010; Zhang et al., 2013)

69 Treelines across the subarctic vegetation belt are largely dominated by conifers,  
70 although deciduous broadleaves occupy 18% of the forest area at latitudes above 60°  
71 across Eurasia (Krankina et al., 2010) and can form the tundra-to-forest transition in  
72 many subarctic regions with oceanic influence (Callaghan et al., 2005). The area of  
73 deciduous broadleaf woodlands is increasing throughout the subarctic region (Hofgaard,  
74 Tømmervik, Rees, & Hanssen, 2013; Rundqvist et al., 2011; Tømmervik et al., 2004;  
75 Wang et al., 2019), following a general trend of increasing deciduous vegetation at  
76 northern high latitudes (Myers-Smith et al., 2011). These vegetation changes are  
77 predicted to continue in the future (Mekonnen, Riley, Randerson, Grant, & Rogers,  
78 2019) and may cause substantial land-climate feedbacks mediated by changes in albedo,  
79 in carbon sequestration and in evaporative fluxes (Bonan, 2008; Bonfils et al., 2012).  
80 Higher transpiration rates by deciduous broadleaf forests could lead to stronger  
81 evaporative cooling locally (Chapin et al., 2000), although, in a regional context, the  
82 effects of the expansion of deciduous broadleaf trees into the tundra zone can be more  
83 complex and actually enhance Arctic warming (Swann et al., 2010). Moreover,  
84 increased soil moisture uptake by deciduous trees could lead to faster depletion of  
85 snowmelt water during the shoulder season, triggering further hydrological changes  
86 (Young-Robertson, Bolton, Bhatt, Cristóbal, & Thoman, 2016). Therefore, a greater  
87 understanding of the magnitudes and controls of evapotranspiration in deciduous  
88 woodlands is needed to predict future changes in land-atmosphere interactions in  
89 subarctic forest-tundra ecotones.

90 Syntheses addressing magnitudes and drivers of ecosystem evapotranspiration ( $ET_{eco}$ ) at  
91 northern high latitudes show a paucity of data for deciduous broadleaf forests from  
92 subarctic locations (Brümmer et al., 2011; Kasurinen et al., 2014; McFadden, Eugster,  
93 & Chapin III, 2003). These syntheses show that leaf area index (LAI), meteorological  
94 conditions and physiological regulation by vegetation are the three major factors  
95 affecting  $ET_{eco}$  in northern high-latitude ecosystems. In these ecosystems,  
96 evapotranspiration is largely driven by vapour pressure deficit (VPD), radiation and  
97 temperature, with soil moisture often playing a minor role (Beringer, Chapin,  
98 Thompson, & McGuire, 2005; Brümmer et al., 2011). In deciduous forests, growing  
99 season duration also affects seasonal evapotranspiration through the influence on LAI  
100 phenology (Brümmer et al., 2012). Deciduous broadleaf forests from northern high  
101 latitudes show higher evapotranspiration rates compared to conifer forests in the same  
102 region (Brümmer et al., 2011; Kasurinen et al., 2014), but they may also display a  
103 stronger stomatal control with increasing VPD (Welp, Randerson, & Liu, 2007).  
104 However, to what extent do these patterns in the drivers of  $ET_{eco}$  from northern high-  
105 latitude deciduous forests reflect the transpiration regulation by the main canopy?

106 The partitioning of  $ET_{eco}$  into transpiration and evaporation and the factors controlling  
107 this partitioning are still poorly known (Schlesinger & Jasechko, 2014). Subarctic and  
108 northern boreal woodlands typically show a low LAI of the dominant canopy species,  
109 meaning that the contribution of understorey and soil evaporation to ecosystem  
110 evapotranspiration may be moderate to high (Blanken et al., 2001; Iida et al., 2009;  
111 Lafleur, 1992), although it will depend on vegetation structure (Beringer et al., 2005).  
112 This substantial contribution of the soil and understorey to  $ET_{eco}$  implies that eddy flux-  
113 based estimates of  $ET_{eco}$  in these forests may well represent the mix of physical and  
114 biological controls on evaporative fluxes and will only partially capture the  
115 physiological regulation exerted by the main canopy (Ikawa et al., 2015; Kasurinen et  
116 al., 2014). Evaporative fluxes of overstorey, understorey and the forest floor may have  
117 contrasting hydroclimatic responses (Iida et al., 2009) and a strong seasonal variation  
118 (Blanken et al., 2001). Although several studies have addressed the magnitudes and  
119 drivers of the different components of  $ET_{eco}$  in northern boreal and subarctic forests  
120 (Blanken et al., 2001; Grelle, Lundberg, Lindroth, Morén, & Cienciala, 1997; Iida et al.,

121 2009; Ikawa et al., 2015), we are not aware of any study of these characteristics from  
122 subarctic deciduous woodlands.

123 In this article, we quantify the magnitude and seasonal controls on  $ET_{eco}$  and on the  
124 transpiration of the main canopy in two deciduous broadleaf woodlands dominated by  
125 mountain birch (*Betula pubescens* ssp. *czerepanovii* (Orlova) Hamet- Ahti). This is a  
126 representative species of subarctic woodlands covering 600000 ha throughout northern  
127 Fennoscandia (Haapanala et al., 2009). The Abisko site (N Sweden) displays a denser  
128 birch woodland compared to the sparser Kevo site (N Finland), which is also slightly  
129 colder and wetter. Therefore, the Abisko woodland would be representative of denser  
130 canopies which are becoming common across the subarctic in response to warming and  
131 reduced browsing (Callaghan et al., 2013). In both sites, we measured  $ET_{eco}$  and birch  
132 transpiration per leaf area ( $T_{leaf}$ ), which was upscaled to the birch canopy level ( $T_{birch}$ ).  
133 Our main goals were: (1) to identify the drivers of  $ET_{eco}$  and  $T_{leaf}$ , to understand the  
134 environmental controls between the two scales (ecosystem vs branch) and at sites,  
135 which differed substantially in stand structure (denser in Abisko, sparser in Kevo); and  
136 (2) to investigate how variation in canopy structure affects growing season values of  
137  $ET_{eco}$  relative to growing season precipitation and to quantify the contribution of  $T_{birch}$   
138 to  $ET_{eco}$ . To further understand this evapotranspiration partitioning in subarctic  
139 deciduous woodlands, at Kevo we also upscaled evaporative fluxes from birch and  
140 understorey ( $ET_{upscaled}$ ) to explore how this variable compares to  $ET_{eco}$ .

141

## 142 2. Methodology

### 143 2.1. Study sites

144 Two mountain birch (*Betula pubescens* ssp. *czerepanovii*) forest sites within the  
145 northern Fennoscandia sub-Artic vegetation belt were chosen for this study: Abisko  
146 (northern Sweden) and Kevo (northern Finland). Both sites were located near the  
147 mountain birch/tundra ecotone, where mountain birches are polycormic because of the  
148 harsh environmental conditions and the frequent defoliation by autumn and winter  
149 moths (*Epirrita autumnata* and *Operophtera brumata*). At both sites, we measured  
150 transpiration of mountain birch branches, ecosystem evapotranspiration and other

151 environmental drivers during the mountain birch leaf-on period, hereby abbreviated as  
152 ‘growing season’, of 2007 (Abisko, DOY 153-241) and of 2008 (Kevo, DOY 171-257).

153 In Abisko (Figure 1a), measurements were undertaken at a location (68.326°N,  
154 18.833°E, 519 m.a.s.l.) ca. 3.2 km south-east of the Abisko Research Station. At the  
155 study site, mean annual temperature is -0.9°C and mean annual precipitation is 335 mm  
156 (1980-2010, temperature corrected assuming a lapse rate of 0.55 °C per 100 m of  
157 elevation). The predominant substrate is coarse glacial till and soils are typically micro-  
158 podzols, with no permafrost present (Hartley, Hopkins, Sommerkorn, & Wookey,  
159 2010). The landscape presents a relatively complex topography, which results in highly  
160 variable forest cover (Nyström, Holmgren, & Olsson, 2012) and stand structures (Table  
161 1). Understorey vegetation is dominated by the dwarf shrubs *Empetrum nigrum* ssp  
162 *hermaphroditum*, *Vaccinium myrtillus* and *Vaccinium uliginosum* (Hartley et al., 2010;  
163 Poyatos, Gornall, Mencuccini, Huntley, & Baxter, 2012).

164 In Kevo (Figure 1b), measurements were undertaken at a location (69.492°N, 27.234°E,  
165 260 m.a.s.l.) ca. 40 km south of the Kevo Subarctic Research Institute. Climate at the site  
166 (1978-2007, data from the the Kevo Institute station, corrected for lapse rate) is colder  
167 and wetter than in Abisko (-2.4°C and 422 mm mean annual temperature and  
168 precipitation, respectively) and the substrate is composed of gneiss covered by glacial  
169 till, and no permafrost is present at the forest site. Mountain birch forests in Kevo,  
170 located upon gentle slopes/ridges and surrounded by mires in topographically depressed  
171 areas, were sparser and showed a more homogeneous structure compared to Abisko  
172 (Table 1). Understorey vegetation showed a higher LAI compared to Abisko (Table 1);  
173 it consisted of *E. nigrum* below mountain birch canopies and distinct patches covered  
174 by *Betula nana* L. and *Cladonia* spp, lichens in the open areas (Poyatos et al., 2012).

175

176 One forest inventory was established in the vicinity of each of the branch bags sites to  
177 quantify stand structure at the plot level (a 10-m circular plot in Abisko and a 30 x 30 m  
178 plot in Kevo). Another set of 30 x 30 m plots was measured in Abisko (N = 5) and Kevo  
179 (N = 7) to quantify ecosystem-level stand structure and maximum leaf area index,  
180 LAI<sub>max</sub> (m<sup>2</sup> leaf m<sup>-2</sup>ground). Forest inventory plots were at an average distance from the  
181 eddy flux tower of 105 m in Abisko and 450 m in Kevo. Diameters and heights of all

182 stems with diameter at breast height DBH>12 mm within the plots were measured in  
183 2007 at Abisko and in 2008 at Kevo. For Abisko, we used published allometric  
184 equations predicting leaf biomass from stem basal area and height (Dahlberg, Berge,  
185 Petersson, & Vencatasawmy, 2004) to convert leaf biomass supported by each stem into  
186 leaf area using site-specific leaf mass per area. For Kevo, we harvested N = 15 stems  
187 during the peak growing season in 2008, to measure their leaf area and we obtained site-  
188 specific allometries between stem diameter and leaf area (Table S1). Understorey  
189 LAI<sub>max</sub> was obtained from 1 m<sup>2</sup> vegetation surveys (N = 5) in each of the sites,  
190 following Fletcher et al. (2012).

## 191 2.2. Branch-level transpiration measurements

192 At both sites, we selected eight mountain birch branches representative of low and mid-  
193 canopy conditions for branch transpiration measurements. Branch transpiration was  
194 measured using a multiplexed branch bag device based on the closed system approach  
195 (Rayment & Jarvis, 1999; Wingate, Seibt, Moncrieff, Jarvis, & Lloyd, 2007). This  
196 system measures water vapour concentration changes within eight 0.11 m<sup>3</sup> ventilated  
197 cuvettes enclosing individual branches during 7.5 minutes. Branches were measured  
198 sequentially, and a measurement cycle of all eight branches was completed within an  
199 hour. During each measurement period, air temperature, T (°C), relative humidity, RH  
200 (%), and photosynthetically active radiation, PAR (μmols photons m<sup>-2</sup> s<sup>-1</sup>), were  
201 recorded every 5 seconds by a datalogger. The system also recorded the value of  
202 environmental variables at the beginning of each transpiration observation (i.e. hourly).  
203 The subscript 'branch' was used to refer to branch-level meteorological variables  
204 (PAR<sub>branch</sub>, VPD<sub>branch</sub>). Further technical details of the branch bags system and of the  
205 calculation of branch-level transpiration can be found in the Supporting Information S2.

206 We quantified branch transpiration on a leaf area basis,  $T_{leaf}$  (l m<sup>-2</sup> hour<sup>-1</sup>), by dividing  
207 whole-branch transpiration by the leaf area of the branch within the bag. To account for  
208 seasonal variation in branch leaf area, we periodically counted the number of leaves  
209 inside the bags during the growing season. We then multiplied the leaf counts by an  
210 estimation of the average leaf area obtained from a sample of leaves (N = 10) close to  
211 the measured branch, fitted a nonlinear response as a function of day of year and, if  
212 needed, corrected by differences in leaf size between inside and outside the bags



213 (Poyatos et al., 2012). We expressed the seasonal variation in leaf area in relative terms  
214 between 0 and 1 (minimum and maximum leaf area, respectively) to use for the  
215 upscaling of branch transpiration fluxes.

### 216 2.3. *Ecosystem evapotranspiration and environmental monitoring*

217 At both sites, half-hourly ecosystem evapotranspiration,  $ET_{eco}$  ( $\text{mm h}^{-1}$ ), was estimated  
218 from latent heat measurements using the eddy covariance (EC) technique in flux towers  
219 located above the mountain birch canopy (Aubinet, Vesala, & Papale, 2012). The three  
220 components of wind speed were measured with a sonic anemometer (R3, Gill  
221 Instruments, Lymington, UK) and water vapour concentrations were measured by an  
222 open-path infrared gas analyser (LI-7500, LI-COR Biosciences, Lincoln, USA). Raw  
223 data were logged at 20 Hz and processed to 30-minute statistics using FluxView (Centre  
224 for Ecology and Hydrology, Wallingford, UK) and quality-controlled following  
225 standard procedures. These include correcting sonic data for angle-of-attack (Gash &  
226 Dolman, 2003), compensating for the lag time between sonic and gas analyser, rotating  
227 the co-ordinate system (so that the horizontal wind vector is aligned with the 30-min  
228 mean and the vertical component is forced to zero), correcting sonic temperature for  
229 humidity (Schotanus, Nieuwstadt, & De Bruin, 1983), correcting the fluxes for high-  
230 and low- frequency spectral losses and correcting gas fluxes for density effects (Webb,  
231 Pearman, & Leuning, 1980). Quality control involved despiking and removal of data  
232 outside physically reasonable limits, when instruments malfunctioned, when the  
233 windows of the gas analyser were wet or dirty, and during periods of heavy rain.  
234 Filtering of data during low turbulence conditions based on a friction velocity threshold  
235 was not applied. Energy balance closure was within the expected range (Stoy et al.,  
236 2013) and did not differ much across sites (Supplementary Information S3).

237 Meteorological stations installed at the flux towers measured half-hourly values of  
238 temperature, relative humidity, PAR and precipitation above the birch canopy and we  
239 refer to them using the subscript 'eco' ( $PAR_{eco}$ ,  $VPD_{eco}$ ). Soil volumetric water content  
240 in the upper 30 cm of the soil, SWC ( $\text{cm}^3 \text{cm}^{-3}$ ), was measured with 1 or 2 frequency  
241 domain reflectometers (CS616, Campbell Scientific, UK) at each site. To account for  
242 site-specific differences in maximum and minimum water-holding capacity, we



transformed SWC into soil moisture deficit (SMD), which ranged from 0 (maximum soil moisture) to 1 (minimum soil moisture) (Granier & Loustau, 1994).

#### 2.4. Modelling environmental controls of evaporative fluxes

Firstly,  $T_{leaf}$  and  $ET_{eco}$  data were filtered ( $PAR > 50 \mu\text{mol photons m}^{-2} \text{ s}^{-1}$ ) to avoid noisy vapour concentration data in the branch bags and low turbulence conditions in the case of EC. For  $T_{leaf}$ , the values of the meteorological drivers were measured locally in each individual branch ( $VPD_{branch}$ ,  $PAR_{branch}$ ) and for  $ET_{eco}$  they were measured above the canopy ( $VPD_{eco}$ ,  $PAR_{eco}$ ).

All models were fitted using the nlme package (Pinheiro, Bates, DebRoy, Sarkar, & R Core Team, 2018) in R (R Core Team 2016).  $T_{leaf}$  was modelled using a linear mixed effects model (lme), with  $VPD_{branch}$ ,  $PAR_{branch}$  and SMD as fixed factors and  $ET_{eco}$  was fitted as a function of  $VPD_{eco}$ ,  $PAR_{eco}$  and SMD using a generalized least squares model (gls). In view of the residual distributions after preliminary analyses, we log-transformed the response variables,  $T_{leaf}$  and  $ET_{eco}$ , and the explanatory variables, except for the case of PAR in  $ET_{eco}$  modelling. All models included a first-order autoregressive correlation structure for the residuals, specifying fractional day of year as a continuous time covariate. We applied model selection to include those terms which minimised the value of the Akaike Information Criterion (AIC) while checking that variance inflation factors were below 10 (Zuur, Ieno, & Elphick, 2010). Model selection was carried out with models fitted using maximum likelihood, but final models were fitted using restricted maximum likelihood (Pinheiro & Bates, 2000). Normality, linearity and homoscedasticity of residuals were visually inspected and temporal autocorrelation was analysed visually by autocorrelation plots using the *acf* function in R. We calculated marginal and conditional  $R^2$ , the proportion of variance explained by fixed and by both fixed and random factors, respectively (Nakagawa & Schielzeth, 2013).

#### 2.5. Overstorey contributions to ecosystem evapotranspiration

Before upscaling, evaporative flux data were aggregated at the daily scale, using models obtained in section 2.4 to gap-fill missing hourly data and fitting daily models when meteorological data from the measurement systems were missing (Supporting Information S4). We obtained transpiration of the mountain birch canopy,  $T_{birch}$  (mm day<sup>-1</sup>), by multiplying  $T_{leaf}$  by the LAI of mountain birch in each stand (Table 1),

274 corrected for seasonal variation (see section 2.2). The calculation was done using mean  
275 and  $\pm$  standard error (SE) of the LAI values, to propagate the uncertainty of the LAI  
276 values at each site into the upscaled estimates of  $T_{birch}$ .

277 At both sites we calculated the mountain birch contribution to daily ecosystem  
278 evapotranspiration,  $T_{birch}/ET_{eco}$  (%). We analysed  $T_{birch}/ET_{eco}$  as a separate linear model  
279 of VPD, PAR (both log-transformed) and SMD, including a factor coding for site  
280 (Abisko and Kevo) which interacted with each of the environmental drivers. Model  
281 selection was carried out based on AIC, as described in section 2.4. We also tested for a  
282 possible influence of interception and subsequent canopy evaporation on  $T_{birch}/ET_{eco}$  by  
283 testing for differences between dry and wet days, using a gls model as described in the  
284 previous paragraph. We considered wet days as those within 2 days after a precipitation  
285 event  $> 1$  mm, assuming all wet surfaces would have dried up during this period  
286 (Knauer, Werner, & Zaehle, 2015).

287 Growing season values (mm) of precipitation ( $P$ ),  $T_{birch}$ ,  $ET_{eco}$  and  $ET_{upscaled}$  were  
288 calculated by aggregating daily values. We also quantified the overall growing season  
289 contribution of  $T_{birch}$  and  $ET_{upscaled}$  to  $ET_{eco}$  and expressed growing season evaporative  
290 fluxes as a percentage of growing season precipitation.

## 291 2.6. Upscaling evapotranspiration components in Kevo

292 In Kevo, measurements of evapotranspiration were available for other ecosystem  
293 components, i.e., understory shrubs and lichen (Table S3, Figure 1). These  
294 evapotranspiration measurements were representative of small patches and were  
295 obtained with an automated chamber system (Poyatos et al., 2014) operated during the  
296 2008 growing season, in a forest-mire ecotone ca. 200 m from the flux tower (Figure 1).  
297 Hourly evapotranspiration of 12 tundra plots was calculated similarly to branch bags  
298 fluxes (Supporting Information S5). Because of microclimatic alterations, water vapour  
299 sorption in the tubing system and imperfect chamber sealing the automated chamber  
300 system used here has been reported to underestimates the evaporative fluxes (Cohen et  
301 al., 2015). Therefore, we applied a correction factor of 2.3, obtained in that study, which  
302 used a similar device under comparable environmental conditions (Cohen et al., 2015).

303 Shrub evapotranspiration ( $ET_{shrub}$ ) was estimated as the mean of  $N = 9$  plots (mean  
304  $LAI_{max} \pm SE = 0.77 \pm 0.2$ ) with dwarf tundra vegetation (mainly *Empetrum*

hermaphroditum, *Calluna vulgaris* and *Vaccinium* spp.) while lichen evaporation ( $ET_{lichen}$ ) was calculated as the mean of  $N = 3$  lichen heath plots (Poyatos et al., 2014). We then combined evapotranspiration of the individual components with the fractional covers ( $f$ ) of each component within the footprint of the flux tower. Fractional covers were obtained from aerial photography obtained in August 2008 and subsequent vegetation classification (Hartley et al., 2015). We used a dynamic footprint approach (Hartley et al., 2015) to obtain  $f$  values which varied with atmospheric conditions, although results were comparable to those using a simpler, fixed footprint approach (Figure S4). We calculated  $ET_{upscaled}$  ( $\text{mm day}^{-1}$ ) as the product of the time-variable  $f$  of each component and its corresponding  $T$  or  $ET$  value:

$$ET_{upscaled} = T_{birch} + f_{birch} \cdot ET_{shrub} + f_{shrub} \cdot ET_{shrub} + f_{lichen} \cdot ET_{lichen} \quad (1)$$

Where  $f_{birch}$ ,  $f_{shrub}$  and  $f_{lichen}$  represent the fractional covers of birch forest, understory shrubs and lichen, respectively. This equation assumes that shrubs were also typically present under the birch canopies (cf. section 2.1) and that components other than birch, shrubs and lichen (around 5% of fractional cover, Table S3) behave similarly to shrubs.

### 3. Results

#### 3.1. Temporal variation of environmental variables and evaporative fluxes

Evaporative demand (Figure 2a-d) was higher in Abisko than in Kevo, as shown by higher mean growing season values ( $\pm$  standard deviation, SD) of air temperatures ( $10.5 \pm 3.8$  °C and  $9.5 \pm 3.6$  °C, respectively),  $VPD_{eco}$  ( $0.5 \pm 0.3$  kPa and  $0.3 \pm 0.2$  kPa) and  $PAR_{eco}$  ( $407.0 \pm 170.0 \mu\text{mol m}^{-2} \text{s}^{-1}$  and  $260.4 \pm 130.3 \mu\text{mol m}^{-2} \text{s}^{-1}$ ). Light transmission through the birch canopy was higher in Kevo:  $PAR_{branch}/PAR_{eco}$  was 56% in Kevo compared to 30% in Abisko (Figure 2a,b). This was associated with the larger difference between  $VPD_{branch}$  and  $VPD_{eco}$  (Figure 2c,d) in Kevo (average  $VPD_{branch} - VPD_{eco} = 0.30$  kPa) compared to Abisko (average  $VPD_{branch} - VPD_{eco} = 0.14$  kPa). Kevo also received heavier and more frequent precipitation (Figure 2e,f), resulting in higher total growing season precipitation (167.5 mm) compared to Abisko (126.6 mm).

Both  $T_{leaf}$  and  $ET_{eco}$  tended to be higher in Abisko than in Kevo, on average 50% higher for  $T_{leaf}$  and 62% higher for  $ET_{eco}$ . Their seasonal dynamics were similar and followed

the course of evaporative demand (Figure 2g-j). However, some differences between  $T_{leaf}$  and  $ET_{eco}$  during the early growing season (before DOY 160) were apparent for Abisko. The diurnal cycles of evaporative fluxes and their drivers varied seasonally in both sites (Figure S2, S3), as expected due to the changing daylight hours at these latitudes. Abisko typically presented higher  $ET_{eco}$  and  $T_{leaf}$  except during the late season, when  $T_{leaf}$  was equal for the two sites.

### 3. 2. Modelling environmental controls of evaporative fluxes

$ET_{eco}$  and  $T_{leaf}$  increased with PAR and VPD but the relationship with VPD showed much less scatter (Figure 3). In general,  $T_{leaf}$  and  $ET_{eco}$  at a given value of PAR or VPD were higher for Abisko. Models of  $ET_{eco}$  and  $T_{leaf}$  showed a good predictive ability, with marginal  $R^2$  values  $> 0.7$  (Table 2,3). Model predictors included a negative interaction between PAR and VPD but did not include SMD (Table 2,3). The environmental responses of  $ET_{eco}$  did not vary across sites and we only detected site differences for the intercept and the PAR coefficient in the  $T_{leaf}$  model (Table 2,3). In both models, the interaction between VPD and PAR resulted in complex patterns in the variation of  $T_{leaf}$  and  $ET_{eco}$  (Figure 4). For example, for  $T_{leaf}$ , steeper relationships with  $VPD_{branch}$  were predicted at low  $PAR_{branch}$  in both sites. In Abisko, higher  $ET_{eco}$  was predicted under conditions of high  $PAR_{eco}$  and low  $VPD_{eco}$  values (Figure 4).

### 3. 3. Overstorey and understorey contributions to ecosystem evapotranspiration

Higher spatial variability of LAI in Abisko (Table 1) translated into a much larger variability in  $T_{bitch}$ , while  $T_{bitch}$  was lower and less variable in Kevo (Figure 5). On average, the daily contribution of mean  $T_{bitch}$  to  $ET_{eco}$  reached peak values of *ca.* 65% in Abisko and *ca.* 30% in Kevo. However, the highly variable LAI in Abisko (Table 1) resulted in the upper bound of  $T_{bitch}/ET_{eco}$  occasionally approaching 100% at this location (Figure 5c).

The value of  $T_{bitch}/ET_{eco}$  increased with  $VPD_{eco}$  and  $PAR_{eco}$  (both log-transformed; Table S4, Figure 6a,b). In both cases, model selection retained the interaction between site and the environmental variable, but it was not significant for either driver (Table S4). We did not detect any effect of SMD on  $T_{bitch}/ET_{eco}$  (Figure 6c; Table S4). We did not find any difference in  $T_{bitch}/ET_{eco}$  between dry and wet days ( $p = 0.27$ ).

365 The mean growing season contribution of  $T_{birch}$  to  $ET_{eco}$  was relatively low in Abisko  
366 (ca. 33%) but it was even lower in Kevo (16%, Table 4). Daily evapotranspiration by  
367 understorey components in Kevo was generally lower compared to  $T_{birch}$  (Figure 5d).  
368 For the whole of the growing season,  $ET_{upscaled}$  only amounted to ca. 40% of  $ET_{eco}$  in  
369 Kevo (Table 4).

370 Daily  $ET_{eco}$  was higher in Abisko (Figure 5a,b), which also showed higher growing  
371 season totals compared to Kevo (Table 4). Remarkably, in Abisko  $ET_{eco}$  was 27%  
372 higher than the precipitation in the same period, while in Kevo the ecosystem returned  
373 to the atmosphere only ca. 59% of precipitation ( $ET_{eco}/P$ , Table 4). Nevertheless, the  
374 relative role of mountain birch transpiration in recycling precipitation was much higher  
375 in Abisko than in Kevo ( $T_{birch}/P$ , Table 4).

376

## 377 4. Discussion

### 378 4.1. Differences in seasonal and environmental controls on transpiration and 379 evapotranspiration between sites

380 Boreal and arctic regions are undergoing very rapid and pronounced climatic warming,  
381 which is expected to modify water and energy fluxes across much of the terrestrial  
382 biosphere of these northern regions. We find that controls of evaporative fluxes by  
383 mixed birch-tundra communities of Northern Fennoscandia largely consist of controls  
384 by VPD (which strongly depends on air and canopy temperature) and by PAR. The  
385 relative importance of these effects depended partly on specific site conditions and the  
386 scale (branch versus ecosystem) at which they were considered. Predicted increases in  
387 air temperature can therefore be expected to increase the relative contribution of VPD  
388 relative to PAR in controlling evaporative fluxes.

389 Conversely, we find that the evaporative fluxes are not affected by temporal changes in  
390 soil moisture, suggesting that water supply is currently not a major limiting factor to  
391 evapotranspiration. Thus, there were no edaphic drought stress effects in  $T_{leaf}$  regulation  
392 by mountain birch, confirming results observed for other birch species (Gartner,  
393 Nadezhdina, Englisch, Čermak, & Leitgeb, 2009; Yan et al., 2018). Our results at the  
394 ecosystem level are consistent with field studies in forest-tundra systems (Beringer et

395 al., 2005) and with a recent data synthesis, where no effect of soil moisture was reported  
396 for evapotranspiration at high latitudes (Kasurinen et al., 2014). Nevertheless,  
397 evaporative fluxes in boreal forests in more continental climates, with higher  
398 evaporative demands, may be influenced by soil moisture (Ohta et al., 2008).

399 At the seasonal time scale, fluxes were primarily controlled by LAI dynamics at both  
400 sites (cf. Poyatos et al., 2012). Seasonal courses of  $T_{leaf}$  and  $ET_{eco}$  mirrored each other,  
401 except during the start of the growing season in Abisko, when the discrepancy between  
402  $T_{leaf}$  and  $ET_{eco}$  may have been caused by combined errors in the quantification of low  
403 fluxes and leaf area during early leaf development. Alternatively, this temporal  
404 mismatch between  $T_{leaf}$  and  $ET_{eco}$  may have been driven by substantial evaporation from  
405 moist soils after snowmelt and/or spatial variability in the phenology of greening up  
406 between the measured branches and the rest of the forest.

407 Both  $T_{leaf}$  and  $ET_{eco}$  were higher in Abisko than in Kevo because of the generally higher  
408 evaporative demand in Abisko (Figure 2). Environmental controls on  $T_{leaf}$  were very  
409 similar across sites. The only significant difference in the response of  $T_{leaf}$  to PAR may  
410 be due to differences in stand structure at the plot level (Table 1). The responses of  
411 evaporative fluxes to PAR and VPD differed between the two sites more clearly for  $T_{leaf}$   
412 than for  $ET_{eco}$ , suggesting a higher sensitivity to VPD of the birch canopy compared to  
413 other ecosystem components (see also section 4.2). The negative interaction between  
414 VPD and PAR produced complex response surfaces of evaporative fluxes to  
415 environmental conditions. Model responses during conditions of high evaporative  
416 demand were reasonable, apart from those by  $ET_{eco}$  at Abisko, where the model showed  
417 a decrease of  $ET_{eco}$  with VPD at high PAR. The more extreme responses were found for  
418 unrealistic combinations of environmental conditions, which are not usually found in  
419 the field. (i.e. high VPD and low PAR), and when the model's predictions of the  
420 interaction effects are less reliable.

421

#### 422 4.2. Contribution of mountain birch transpiration to ecosystem evapotranspiration 423 across sites and environmental conditions

424 The mean daily contribution of birch transpiration to ecosystem evapotranspiration (i.e.  
425  $T_{birch}/ET_{eco}$ ) was much higher in Abisko than in Kevo. In Abisko, the higher variability

426 in LAI at the landscape level propagates to a larger range of  $T_{birch}/ET_{eco}$  values  
427 compared to Kevo. When explaining seasonal variability in  $T_{birch}/ET_{eco}$ , we found that  
428  $T_{birch}/ET_{eco}$  strongly depended on VPD and PAR, with  $T_{birch}/ET_{eco}$  saturating at high  
429 VPD, but this environmental control on  $T_{birch}/ET_{eco}$  was stronger in Abisko. Therefore,  
430 our results show an increased relative role of mountain birch in controlling ecosystem  
431 evapotranspiration as evaporative demand increases, especially in denser forests, in  
432 contrast with studies on waterlogged peatlands where understorey contribution increases  
433 with VPD (Ikawa et al., 2015). In our sites, mountain birch roots possibly access soil  
434 moisture at greater depths (Hunziker, Sigurdsson, Halldorsson, Schwanghart, & Kuhn,  
435 2014), supplying water to meet the increasing evaporative demand and causing the  
436 increase in  $T_{birch}/ET_{eco}$ .

437 At the growing season level, birch transpiration contributed *ca.* 33% of total ecosystem  
438 evapotranspiration in Abisko but the contribution was only *ca.* 16% in Kevo (Table 4).  
439 These differences were attributable not only to a higher birch LAI in Abisko (Table 1),  
440 but also to the higher  $T_{leaf}$  values at this site (Figure 2). Lower  $T_{birch}/ET_{eco}$  values in  
441 Kevo could also result from a disproportionately higher contribution from the  
442 understorey in a sparser woodland (i.e. higher below-canopy incident radiation  
443 compared to Abisko). The values of  $T_{birch}/ET_{eco}$  at the two sites are consistent with  
444 the generally low contribution of overstorey to total evapotranspiration in subarctic and  
445 northern boreal forests (Iida et al., 2009; Ikawa et al., 2015; Kelliher et al., 1997;  
446 Lafleur, 1992; Warren et al., 2019). However, in Kevo, our estimates of upscaled  
447 evapotranspiration from individual ecosystem components (i.e. mountain birch,  
448 understorey shrubs and lichen heath) yielded growing season values, which were still  
449 far from total ecosystem evapotranspiration measured by eddy covariance (Table 4, cf.  
450 section 4.3). In the following section, we discuss potential methodological artefacts and  
451 unmeasured processes that could explain this discrepancy.

#### 452 4.3. Methodological considerations

453 This study jointly analyses a multi-scale dataset of evaporative fluxes from subarctic  
454 forest communities. Comparing evaporative fluxes across scales is hindered by the  
455 numerous potential errors associated with measurement techniques and upscaling  
456 procedures. Transpiration measurements from closed chambers could have been



457 affected by radiation-driven overheating (Poyatos et al., 2012), by raising  $VPD_{branch}$   
458 above  $VPD_{eco}$  and causing an overestimation of  $T_{leaf}$ . However, the relatively low values  
459 of  $T_{birch}$  and  $ET_{upscaled}$ , both based on closed chamber measurements, do not suggest that  
460 the conclusions of this study could have been affected by this artefact.

461 The upscaling procedure also has a number of potential limitations that warrant  
462 consideration. Due to the sparseness of the forest in Kevo (i.e. little shading effects on  
463 understorey vegetation), we assumed that the magnitude and regulation of understorey  
464 evapotranspiration was similar to that shown by patches with similar composition in the  
465 forest-tundra transition (Poyatos et al., 2014). However, LAI of the patches measured  
466 with automated chambers in the forest-mire transition (see section 2.5) was *ca.* 50% of  
467 the LAI actually measured in survey plots located within the forest (Table 1). Rescaling  
468 the understorey fluxes according to this understorey LAI, evapotranspiration from  
469 understorey components at the ecosystem level would be amount to 23.6 mm, an  
470 evaporative flux 55% larger than  $T_{birch}$ . Scaling-up evapotranspiration estimated from  
471 canopy and understorey components, accounting for their land cover fractions and  
472 applying the LAI correction outlined above to understorey measurements would  
473 increase growing season  $ET_{upscaled}$  values to 44.4 mm, or *ca.* 45% of  $ET_{eco}$ .

#### 474 4.4. Differences in growing season water balance across sites

475 Even accounting for this likely underestimation of  $ET_{shrub}$  and  $ET_{lichen}$ , there is still a  
476 fraction of  $ET_{eco}$  that cannot be explained by upscaled gas exchange measurements from  
477 individual ecosystem components. Taking into account that  $T_{birch}$  obtained from branch-  
478 bag measurements excludes evaporation of intercepted water, we showed that  
479  $T_{birch}/ET_{eco}$  does not vary between dry and wet days. This may suggest that evaporation  
480 of intercepted water may not be captured by eddy covariance measurements, otherwise  
481  $T_{birch}/ET_{eco}$  would have been lower on wet days than dry days. Potentially high  
482 evaporation rates after precipitation may be partially missed from  $ET_{eco}$  and  $ET_{upscaled}$ ,  
483 because data from open-path gas analysers are removed when the sensor windows are  
484 wet and subsequent gap-filling would not account for the missed evaporation of  
485 intercepted water (Oishi, Oren, & Stoy, 2008). Combined interception by overstorey  
486 canopies and mosses in northern boreal forests may amount up to 40% of bulk

487 precipitation (Price, Dunham, Carleton, & Band, 1997), and we are not currently  
488 accounting for this substantial contribution.

489 We found stark differences between sites in the percentage of precipitation returned to  
490 the atmosphere as evapotranspiration; the mountain birch woodland in Abisko  
491 evaporated more water than it received during the growing season, as observed in other  
492 deciduous boreal forests (Blanken et al., 2001; Kelliher et al., 1997). In contrast, Kevo  
493 showed a substantial water surplus (Table 4). Our measurements did not include the  
494 snowmelt period, but these sites can reach snowpack depths of  $> 1$  m (data for Kevo,  
495 2009) and tree water uptake during this period, especially from deciduous species, can  
496 progressively deplete soil water sources (Young-Robertson et al., 2016). This decline in  
497 soil water content after snowmelt is very clear in the seasonal course of SMD measured  
498 in Abisko in 2008 and 2009 (outside our measurement period in Abisko, Fig S5).  
499 Therefore, these differences in the role of the mountain birch canopy between Abisko  
500 and Kevo, mediated by their different stand structure, can illustrate the potential  
501 changes in the hydrological regime that can result from the expansion and densification  
502 of subarctic deciduous woodlands.

#### 503 *4.5. Concluding remarks*

504 We have shown that the dominant mountain birch canopy plays only a partial role in  
505 driving ecosystem evapotranspiration in both subarctic sites, and this may be a general  
506 feature of low-LAI subarctic and northern boreal forests (Saugier, Granier, Pontailler,  
507 Dufrene, & Baldocchi, 1997). Our results also show that both increased woodland cover  
508 and increased woodland density under climate change conditions (Rundqvist et al.,  
509 2011) will result in larger controls of the water fluxes by the canopies of deciduous trees  
510 as opposed to the understorey vegetation. However, our upscaling exercise also shows  
511 that adequately accounting for understorey components (and transpiration vs  
512 evaporation processes; Stoy et al., 2019) may be necessary to constrain future  
513 hydrological changes in these areas. The highly variable and patchy nature of subarctic  
514 vegetation may require flux upscaling approaches considering spatial variation not only  
515 of land cover (Hartley et al., 2015), but also of LAI (Stoy et al., 2013).

516 In the longer term, shifts towards deciduous-dominated communities in subarctic  
517 regions and an increased land cover by forest as opposed to tundra are expected to

518 induce large hydro-climatic effects. These effects are expected to be mediated by higher  
519 transpiration rates, inducing complex land-climate feedbacks (Bonfils et al., 2012;  
520 Swann et al., 2010), which need to be considered together with carbon- and energy-  
521 related feedbacks (Wit et al., 2014). Overall, combining several flux datasets and land  
522 cover information we provide, for the poorly studied subarctic deciduous woodlands,  
523 highly valuable results that will help to calibrate and validate evapotranspiration  
524 processes in ecosystem models.

## 525 Acknowledgements

526 AM. Sabater is supported by European Social Fund and Generalitat Valenciana (GVA)  
527 under a PhD contract (ACIF – 2017/9830). This study was funded by the following  
528 grants: ABACUS NE/D005795/1 (NERC, UK), SAPFLUXNET CGL2014-JIN-55583  
529 (MINECO, Spain), VERSUS CGL2015-67466-R (MINECO/FEDER), SGR-2017-1001  
530 (AGAUR, Generalitat de Catalunya) and IMAGINA PROMETEU/2019/110  
531 (Conselleria de Cultura, GVA). We are grateful for the support by the staff at the Kevo  
532 Subarctic Research Institute and at the Abisko Research Station. We would also like to  
533 acknowledge the help in the field by T. August, A. Robertson, K. Leslie, D. Sayer and  
534 J.R.M. Allen.

535

## 536 References

- Aubinet, M., Vesala, T., & Papale, D. (2012). *Eddy Covariance: A Practical Guide to Measurement and Data Analysis*. Springer Science & Business Media.
- Beringer, J., Chapin, F. S., Thompson, C. C., & McGuire, A. D. (2005). Surface energy exchanges along a tundra-forest transition and feedbacks to climate. *Agricultural and Forest Meteorology*, 131(3–4), 143–161.
- Blanken, P. D., Black, T. A., Neumann, H. H., den Hartog, G., Yang, P. C., Nesic, Z., & Lee, X. (2001). The seasonal water and energy exchange above and within a boreal aspen forest. *Journal of Hydrology*, 245(1–4), 118–136. [https://doi.org/10.1016/S0022-1694\(01\)00343-2](https://doi.org/10.1016/S0022-1694(01)00343-2)
- Bonan, G. B. (2008). Forests and Climate Change: Forcings, Feedbacks, and the Climate Benefits of Forests. *Science*, 320, 1444–1449. <https://doi.org/10.1126/science.1155121>
- Bonfils, C. J. W., Phillips, T. J., Lawrence, D. M., Cameron-Smith, P., Riley, W. J., & Subin, Z. M. (2012). On the influence of shrub height and expansion on northern high latitude climate. *Environmental Research Letters*, 7(1), 015503. <https://doi.org/10.1088/1748-9326/7/1/015503>

- Brümmer, C., Black, T. A., Jassal, R. S., Grant, N. J., Spittlehouse, D. L., Chen, B., ... Wofsy, S. C. (2011). How climate and vegetation type influence evapotranspiration and water use efficiency in Canadian forest, peatland and grassland ecosystems. *Agricultural and Forest Meteorology*. <https://doi.org/10.1016/j.agrformet.2011.04.008>
- Callaghan, T. V., Björn, L. O., Chapin Iii, F., Chernov, Y., Christensen, T. R., Huntley, B., ... Shaver, G. R. (2005). Arctic tundra and polar desert ecosystems. In *Arctic climate impact assessment* (Vol. 1, pp. 243–352).
- Callaghan, T. V., Jonasson, C., Thierfelder, T., Yang, Z., Hedenås, H., Johansson, M., ... Sloan, V. L. (2013). Ecosystem change and stability over multiple decades in the Swedish subarctic: Complex processes and multiple drivers. *Philosophical Transactions of the Royal Society B: Biological Sciences*, 368(1624), 20120488. <https://doi.org/10.1098/rstb.2012.0488>
- Chapin, F. S., Mcguire, A. D., Randerson, J., Pielke, R., Baldocchi, D., Hobbie, S. E., ... Running, S. W. (2000). Arctic and boreal ecosystems of western North America as components of the climate system. *Global Change Biology*, 6(S1), 211–223. <https://doi.org/10.1046/j.1365-2486.2000.06022.x>
- Cohen, L. R., Raz-Yaseef, N., Curtis, J. B., Young, J. M., Rahn, T. A., Wilson, C. J., ... Newman, B. D. (2015). Measuring diurnal cycles of evapotranspiration in the Arctic with an automated chamber system. *Ecohydrology*, 8(4), 652–659. <https://doi.org/10.1002/eco.1532>
- Dahlberg, U., Berge, T. W., Petersson, H., & Vencatasawmy, C. P. (2004). Modelling biomass and leaf area index in a sub-arctic Scandinavian mountain area. *Scandinavian Journal of Forest Research*, 19, 60–71. <https://doi.org/10.1080/02827580310019266>
- Fletcher, B. J., Gornall, J. L., Poyatos, R., Press, M. C., Stoy, P. C., Huntley, B., ... Phoenix, G. K. (2012). Photosynthesis and productivity in heterogeneous arctic tundra: Consequences for ecosystem function of mixing vegetation types at stand edges. *Journal of Ecology*, 100(2), 441–451. <https://doi.org/10.1111/j.1365-2745.2011.01913.x>
- Gartner, K., Nadezhdina, N., Englisch, M., Čermak, J., & Leitgeb, E. (2009). Sap flow of birch and Norway spruce during the European heat and drought in summer 2003. *Forest Ecology and Management*, 258(5), 590–599. <https://doi.org/10.1016/j.foreco.2009.04.028>
- Gash, J. H. C., & Dolman, A. J. (2003). Sonic anemometer (co)sine response and flux measurement: I. The potential for (co)sine error to affect sonic anemometer-based flux measurements. *Agricultural and Forest Meteorology*, 119(3), 195–207. [https://doi.org/10.1016/S0168-1923\(03\)00137-0](https://doi.org/10.1016/S0168-1923(03)00137-0)
- Granier, A., & Loustau, D. (1994). Measuring and modelling the transpiration of a maritime pine canopy from sap-flow data. *Agricultural and Forest Meteorology*, 71, 61–81.
- Grelle, A., Lundberg, A., Lindroth, A., Morén, A.-S., & Cienciala, E. (1997). Evaporation components of a boreal forest: Variations during the growing season. *Journal of Hydrology*, 197(1), 70–87. [https://doi.org/10.1016/S0022-1694\(96\)03267-2](https://doi.org/10.1016/S0022-1694(96)03267-2)
- Haapanala, S., Ekberg, A., Hakola, H., Tarvainen, V., Rinne, J., Hellén, H., & Arneth, A. (2009). Mountain birch—potentially large source of sesquiterpenes into high latitude atmosphere. *Biogeosciences*, 6, 2709–2718.

- Hartley, I. P., Hopkins, D. W., Sommerkorn, M., & Wookey, P. A. (2010). The response of organic matter mineralisation to nutrient and substrate additions in sub-arctic soils. *Soil Biology and Biochemistry*, 42(1), 92–100.
- Hartley, Iain. P., Hill, Timothy. C., Wade, Thomas. J., Clement, Robert. J., Moncrieff, John. B., Prieto-Blanco, Ana., ... Baxter, Robert. (2015). Quantifying landscape-level methane fluxes in subarctic Finland using a multiscale approach. *Global Change Biology*, 21(10), 3712–3725. <https://doi.org/10.1111/gcb.12975>
- Hofgaard, A., Tømmervik, H., Rees, G., & Hanssen, F. (2013). Latitudinal forest advance in northernmost Norway since the early 20th century. *Journal of Biogeography*, 40(5), 938–949. <https://doi.org/10.1111/jbi.12053>
- Hunziker, M., Sigurdsson, B. D., Halldorsson, G., Schwanghart, W., & Kuhn, N. (2014). Biomass allometries and coarse root biomass distribution of mountain birch in southern Iceland. *Icelandic Agricultural Sciences*, 27, 111–125.
- Iida, S., Ohta, T., Matsumoto, K., Nakai, T., Kuwada, T., Kononov, A. V., ... Yabuki, H. (2009). Evapotranspiration from understory vegetation in an eastern Siberian boreal larch forest. *Agricultural and Forest Meteorology*, 149(6), 1129–1139. <https://doi.org/10.1016/j.agrformet.2009.02.003>
- Ikawa, H., Nakai, T., Busey, R. C., Kim, Y., Kobayashi, H., Nagai, S., ... Hinzman, L. (2015). Understory CO<sub>2</sub>, sensible heat, and latent heat fluxes in a black spruce forest in interior Alaska. *Agricultural and Forest Meteorology*, 214–215, 80–90. <https://doi.org/10.1016/j.agrformet.2015.08.247>
- IPCC. (2013). *Climate Change 2013: The Physical Science Basis. Contribution of Working Group I to the Fifth Assessment Report of the Intergovernmental Panel on Climate Change*. <https://doi.org/10.1017/CBO9781107415324>
- Kasurinen, V., Alfredsen, K., Kolari, P., Mammarella, I., Alekseychik, P., Rinne, J., ... Berninger, F. (2014). Latent heat exchange in the boreal and arctic biomes. *Global Change Biology*, 20(11), 3439–3456. <https://doi.org/10.1111/gcb.12640>
- Kattsov, V. M., Källén, E., Cattle, H. P., Christensen, J., Drange, H., Hanssen-Bauer, I., ... others. (2005). *Future climate change: Modeling and scenarios for the Arctic*.
- Kelliher, F. M., Hollinger, D. Y., Schulze, E.-D., Vygodskaya, N. N., Byers, J. N., Hunt, J. E., ... Bauer, G. (1997). Evaporation from an eastern Siberian larch forest. *Agricultural and Forest Meteorology*, 85(3), 135–147. [https://doi.org/10.1016/S0168-1923\(96\)02424-0](https://doi.org/10.1016/S0168-1923(96)02424-0)
- Knauer, J., Werner, C., & Zaehle, S. (2015). Evaluating stomatal models and their atmospheric drought response in a land surface scheme: A multibiome analysis. *Journal of Geophysical Research: Biogeosciences*, 120(10), 2015JG003114. <https://doi.org/10.1002/2015JG003114>
- Krankina, O. N., Pflugmacher, D., Hayes, D. J., McGuire, A. D., Hansen, M. C., Häme, T., ... Nelson, P. (2010). Vegetation cover in the eurasian arctic: Distribution, monitoring, and role in carbon cycling. In *Eurasian arctic land cover and land use in a changing climate* (pp. 79–108). Springer.
- Lafleur, P. M. (1992). Energy balance and evapotranspiration from a subarctic forest. *Agricultural and Forest Meteorology*, 58(3–4), 163–175. [https://doi.org/10.1016/0168-1923\(92\)90059-D](https://doi.org/10.1016/0168-1923(92)90059-D)
- McFadden, J. P., Eugster, W., & Chapin III, F. S. (2003). A regional study of the controls on water vapor and CO<sub>2</sub> exchange in arctic tundra. *Ecology*, 84(10), 2762–2776.



- Mekonnen, Z. A., Riley, W. J., Randerson, J. T., Grant, R. F., & Rogers, B. M. (2019). Expansion of high-latitude deciduous forests driven by interactions between climate warming and fire. *Nature Plants*, 1–7. <https://doi.org/10.1038/s41477-019-0495-8>
- Myers-Smith, I. H., Forbes, B. C., Wilmsking, M., Hallinger, M., Lantz, T., Blok, D., ... Hik, D. S. (2011). Shrub expansion in tundra ecosystems: Dynamics, impacts and research priorities. *Environmental Research Letters*, 6(4), 045509. <https://doi.org/10.1088/1748-9326/6/4/045509>
- Nakagawa, S., & Schielzeth, H. (2013). A general and simple method for obtaining R<sup>2</sup> from generalized linear mixed-effects models. *Methods in Ecology and Evolution*, 4(2), 133–142. <https://doi.org/10.1111/j.2041-210x.2012.00261.x>
- Nyström, M., Holmgren, J., & Olsson, H. (2012). Prediction of tree biomass in the forest–tundra ecotone using airborne laser scanning. *Remote Sensing of Environment*, 123, 271–279. <https://doi.org/10.1016/j.rse.2012.03.008>
- Ohta, T., Maximov, T. C., Dolman, A. J., Nakai, T., van der Molen, M. K., Kononov, A. V., ... Yabuki, H. (2008). Interannual variation of water balance and summer evapotranspiration in an eastern Siberian larch forest over a 7-year period (1998–2006). *Agricultural and Forest Meteorology*, 148(12), 1941–1953. <https://doi.org/10.1016/j.agrformet.2008.04.012>
- Oishi, A. C., Oren, R., & Stoy, P. C. (2008). Estimating components of forest evapotranspiration: A footprint approach for scaling sap flux measurements. *Agricultural and Forest Meteorology*, 148(11), 1719–1732.
- Pinheiro, J., Bates, D., DebRoy, S., Sarkar, D., & R Core Team. (2018). *nlme: Linear and Nonlinear Mixed Effects Models*. Retrieved from <https://CRAN.R-project.org/package=nlme>
- Poyatos, R., Gornall, J., Mencuccini, M., Huntley, B., & Baxter, R. (2012). Seasonal controls on net branch CO<sub>2</sub> assimilation in sub-Arctic Mountain Birch (*Betula pubescens* ssp. *Czerepanovii* (Orlova) Hamet-Ahti). *Agricultural and Forest Meteorology*, 158–159, 90–100. <https://doi.org/10.1016/j.agrformet.2012.02.009>
- Poyatos, R., Heinemeyer, A., Ineson, P., Evans, J. G., Ward, H. C., Huntley, B., & Baxter, R. (2014). Environmental and Vegetation Drivers of Seasonal CO<sub>2</sub> Fluxes in a Sub-arctic Forest–Mire Ecotone. *Ecosystems*, 17(3), 377–393. <https://doi.org/10.1007/s10021-013-9728-2>
- Price, A. G., Dunham, K., Carleton, T., & Band, L. (1997). Variability of water fluxes through the black spruce (*Picea mariana*) canopy and feather moss (*Pleurozium schreberi*) carpet in the boreal forest of Northern Manitoba. *Journal of Hydrology*, 196(1), 310–323. [https://doi.org/10.1016/S0022-1694\(96\)03233-7](https://doi.org/10.1016/S0022-1694(96)03233-7)
- Rayment, M. B., & Jarvis, P. G. (1999). Seasonal gas exchange of black spruce using an automatic branch bag system. *Canadian Journal of Forest Research*, 29, 1528–1538.
- Rundqvist, S., Hedenås, H., Sandström, A., Emanuelsson, U., Eriksson, H., Jonasson, C., & Callaghan, T. V. (2011). Tree and Shrub Expansion Over the Past 34 Years at the Tree-Line Near Abisko, Sweden. *AMBIO: A Journal of the Human Environment*, 40(6), 683–692. <https://doi.org/10.1007/s13280-011-0174-0>
- Saugier, B., Granier, A., Pontailier, J. Y., Dufrene, E., & Baldocchi, D. D. (1997). Transpiration of a boreal pine forest measured by branch bag, sap flow and micrometeorological methods. *Tree Physiology*, 17, 511–519.

- Schlesinger, W. H., & Jasechko, S. (2014). Transpiration in the global water cycle. *Agricultural and Forest Meteorology*, 189–190, 115–117. <https://doi.org/10.1016/j.agrformet.2014.01.011>
- Schotanus, P., Nieuwstadt, F. T. M., & De Bruin, H. A. R. (1983). Temperature measurement with a sonic anemometer and its application to heat and moisture fluxes. *Boundary-Layer Meteorology*, 26(1), 81–93. <https://doi.org/10.1007/BF00164332>
- Stoy, P. C., Williams, M., Evans, J. G., Prieto-Blanco, A., Disney, M., Hill, T. C., ... Street, L. E. (2013). Upscaling tundra CO<sub>2</sub> exchange from chamber to eddy covariance tower. *Arctic, Antarctic, and Alpine Research*, 45(2), 275–284.
- Stoy, Paul C., El-Madany, T. S., Fisher, J. B., Gentine, P., Gerken, T., Good, S. P., ... Wolf, S. (2019). Reviews and syntheses: Turning the challenges of partitioning ecosystem evaporation and transpiration into opportunities. *Biogeosciences*, 16(19), 3747–3775. <https://doi.org/10.5194/bg-16-3747-2019>
- Stoy, Paul C., Mauder, M., Foken, T., Marcolla, B., Boegh, E., Ibrom, A., ... Varlagin, A. (2013). A data-driven analysis of energy balance closure across FLUXNET research sites: The role of landscape scale heterogeneity. *Agricultural and Forest Meteorology*, 171–172, 137–152. <https://doi.org/10.1016/j.agrformet.2012.11.004>
- Swann, A. L., Fung, I. Y., Levis, S., Bonan, G. B., & Doney, S. C. (2010). Changes in Arctic vegetation amplify high-latitude warming through the greenhouse effect. *Proceedings of the National Academy of Sciences*, 107(4), 1295–1300. <https://doi.org/10.1073/pnas.0913846107>
- Tømmervik, H., Johansen, B., Tombre, I., Thannheiser, D., Høgda, K. A., Gaare, E., & Wielgolaski, F. E. (2004). Vegetation Changes in the Nordic Mountain Birch Forest: The Influence of Grazing and Climate Change. *Arctic, Antarctic, and Alpine Research*, 36(3), 323–332.
- Wang, J. A., Sulla-Menashe, D., Woodcock, C. E., Sonnentag, O., Keeling, R. F., & Friedl, M. A. (2019). Extensive land cover change across Arctic–Boreal Northwestern North America from disturbance and climate forcing. *Global Change Biology*, 0(0). <https://doi.org/10.1111/gcb.14804>
- Warren, R. K., Pappas, C., Helbig, M., Chasmer, L. E., Berg, A. A., Baltzer, J. L., ... Sonnentag, O. (2019). Minor contribution of overstorey transpiration to landscape evapotranspiration in boreal permafrost peatlands. *Ecohydrology*, 11(5), e1975. <https://doi.org/10.1002/eco.1975>
- Webb, E. K., Pearman, G. I., & Leuning, R. (1980). Correction of flux measurements for density effects due to heat and water vapour transfer. *Quarterly Journal of the Royal Meteorological Society*, 106(447), 85–100. <https://doi.org/10.1002/qj.49710644707>
- Welp, L. R., Randerson, J. T., & Liu, H. P. (2007). The sensitivity of carbon fluxes to spring warming and summer drought depends on plant functional type in boreal forest ecosystems. *Agricultural & Forest Meteorology*, 147(3–4), 172–185.
- Wingate, L., Seibt, U., Moncrieff, J. B., Jarvis, P. G., & Lloyd, J. (2007). Variations in  $\delta^{13}\text{C}$  discrimination during CO<sub>2</sub> exchange by *Picea sitchensis* branches in the field. *Plant, Cell & Environment*, 30(5), 600–616. <https://doi.org/10.1111/j.1365-3040.2007.01647.x>
- Wit, H. A. de, Bryn, A., Hofgaard, A., Karstensen, J., Kvilevåg, M. M., & Peters, G. P. (2014). Climate warming feedback from mountain birch forest expansion:



- Reduced albedo dominates carbon uptake. *Global Change Biology*, 20(7), 2344–2355. <https://doi.org/10.1111/gcb.12483>
- Yan, C., Wang, B., Zhang, Y., Zhang, X., Takeuchi, S., & Qiu, G. (2018). Responses of Sap Flow of Deciduous and Conifer Trees to Soil Drying in a Subalpine Forest. *Forests*, 9(1), 32. <https://doi.org/10.3390/f9010032>
- Young-Robertson, J. M., Bolton, W. R., Bhatt, U. S., Cristóbal, J., & Thoman, R. (2016). Deciduous trees are a large and overlooked sink for snowmelt water in the boreal forest. *Scientific Reports*, 6, srep29504. <https://doi.org/10.1038/srep29504>
- Zhang, W., Miller, P. A., Smith, B., Wania, R., Koenigk, T., & Döscher, R. (2013). Tundra shrubification and tree-line advance amplify arctic climate warming: Results from an individual-based dynamic vegetation model. *Environmental Research Letters*, 8(3), 034023. <https://doi.org/10.1088/1748-9326/8/3/034023>
- Zuur, A. F., Ieno, E. N., & Elphick, C. S. (2010). A protocol for data exploration to avoid common statistical problems. *Methods in Ecology and Evolution*, 1(1), 3–14. <https://doi.org/10.1111/j.2041-210X.2009.00001.x>

537 **Tables**

538 **Table 1.** Stand characteristics of mountain birch forests in Abisko and Kevo. Values  
 539 labelled as ‘Site’ represent the site mean ( $\pm$ SE) of all inventory plots in Abisko (N=6)  
 540 and Kevo (N=8). Values labelled as ‘BB’ are the values of the plots in the vicinity of  
 541 the branch bags measuring sites. Tree density refers to polycormic individuals, with  
 542 multiple stems per tree.

	Tree density (trees ha <sup>-1</sup> )	Stems per tree	Basal area (m <sup>2</sup> ha <sup>-1</sup> )	DBH (mm)	Height (m)	Overstorey LAI <sub>max</sub> (m <sup>2</sup> m <sup>-2</sup> )	Understorey LAI <sub>max</sub> (m <sup>2</sup> m <sup>-2</sup> )
Abisko							
Site	1260 $\pm$ 80	3.7 $\pm$ 0.2	6.5 $\pm$ 0.2	36.9 $\pm$ 1.0	3.9 $\pm$ 0.2	1.2 $\pm$ 0.3	1.0 $\pm$ 0.2
BB	1146	4.4	6.7	35.7	-	1.8	-
Kevo							
Site	876 $\pm$ 85	3.3 $\pm$ 0.2	3.8 $\pm$ 0.4	37.2 $\pm$ 2.0	3.8 $\pm$ 0.0	0.7 $\pm$ 0.1	1.5 $\pm$ 0.1
BB	833	3.8	3.0	30.6	3.8	0.6	-

543

544 **Table 2.** Summary statistics of the linear mixed model of log-transformed  $T_{leaf}$  as a  
545 function of environmental variables ( $VPD_{branch}$ ,  $PAR_{branch}$  and SMD) for Abisko and  
546 Kevo. Asterisks denote significant differences from zero ( $*p<0.05$ ,  $**p<0.01$ ,  
547  $***p<0.001$ ). Statistical differences in model coefficients ( $p < 0.05$ ) between Abisko and  
548 Kevo were marked in bold. SD: Standard deviation. Interactions between variables are  
549 denoted by colon ( : ) and variables not included after model selection are denoted by  
550 ‘n.i.’.

	Abisko	Kevo
Fixed effects		
Intercept	<b><math>-2.98 \pm 0.09^*</math></b>	<b><math>-4.00 \pm 0.07^{***}</math></b>
$\log(VPD_{branch})$	$1.26 \pm 0.01^{***}$	$1.27 \pm 0.01^{***}$
$PAR_{branch}$	<b><math>4.1 \cdot 10^{-4} \pm 0.4 \cdot 10^{-4}^{***}</math></b>	<b><math>7.5 \cdot 10^{-4} \pm 0.4 \cdot 10^{-4}^{***}</math></b>
$\log(VPD_{branch}): PAR_{branch}$	$-8.4 \cdot 10^{-4} \pm 0.5 \cdot 10^{-4}^{***}$	$-9.4 \cdot 10^{-4} \pm 0.4 \cdot 10^{-4}^{***}$
SMD	n.i.	n.i.
Random effects (branch)		
SD (Intercept)	0.26	0.20
Residual error	0.40	0.48
Correlation structure ( $\phi$ )	$4.40 \cdot 10^{-8}$	$7.23 \cdot 10^{-7}$
$R^2$ marginal ( $R^2$ conditional)	0.78 (0.84)	0.77 (0.80)

551

552 **Table 3.** Summary statistics of the generalised least squares model of  $ET_{eco}$  as a  
553 function of environmental variables ( $VPD_{eco}$ ,  $PAR_{eco}$  and SMD) for Abisko and Kevo.  
554 Asterisks denote significant differences from zero (\* $p < 0.05$ , \*\* $p < 0.01$ , \*\*\* $p < 0.001$ ). No  
555 significant differences ( $p < 0.05$ ) were found between model coefficients between  
556 Abisko and Kevo. Interactions between variables are denoted by colon ( : ) and  
557 variables not included after model selection are denoted by 'n.i'.

	Abisko	Kevo
Intercept	$-4.93 \pm 0.38^{***}$	$-4.84 \pm 0.40^{***}$
$\log(VPD)$	$2.58 \pm 0.30^{***}$	$2.13 \pm 0.27^{***}$
$\log(PAR_{eco})$	$0.47 \pm 0.06^{***}$	$0.47 \pm 0.06^{***}$
$\log(VPD_{eco}):\log(PAR_{eco})$	$-0.39 \pm 0.05^{***}$	$-0.26 \pm 0.05^{***}$
SMD	n.i.	n.i.
Correlation structure ( $\varphi$ )	$8.23 \cdot 10^{-3}$	$1.84 \cdot 10^{-2}$
$R^2$ marginal	0.71	0.69

558

559

**Table 4.** Growing season values of precipitation ( $P$ ), birch transpiration ( $T_{birch}$ ) and ecosystem evapotranspiration ( $ET_{eco}$ ) in Abisko and Kevo. Percentage of evaporative fluxes as a fraction of  $ET_{eco}$  and  $P$  are also shown for growing season values. Values with an uncertainty measure represent means  $\pm$  standard error.

564  
565

	Abisko	Kevo
$T_{birch}$ (mm)	$52.5 \pm 13.0$	$15.2 \pm 1.5$
$ET_{eco}$ (mm)	160.5	98.5
$ET_{upscaled}$ (mm)	-	$39.4 \pm 1.5$
$T_{birch} / ET_{eco}$ (%)	$32.7 \pm 8.1$	$15.5 \pm 1.5$
$T_{birch} / P$ (%)	$41.4 \pm 10.2$	$9.1 \pm 0.9$
$ET_{eco} / P$ (%)	126.6	58.8
$ET_{upscaled} / ET_{eco}$ (%)	-	$40.0 \pm 1.5$

566

## 567 Figure captions

568 **Figure 1.** Study sites at Abisko (a) and Kevo (b), showing the locations of the branch  
569 bags systems, the eddy flux towers and the understory automated chambers at Kevo.  
570 Panel (a) shows the aerial photography obtained in Abisko and (b) shows the land  
571 classification at Kevo obtained from aerial photography (cf. Hartley et al., 2015). *Birch*  
572 : mountain birch woodland; *Understorey*: low- and dwarf-shrubs; *Lichen*: lichen heath;  
573 *Mire*: organic hummocks and interhummocks with shrubs and *Spahgnum*; *Water*: open  
574 water; *Lawns*: graminoid lawns; *Board*: boardwalks; *Other*: other land cover.

575 **Figure 2.** Seasonal course of environmental variables and evaporative fluxes (daily  
576 means) in Abisko and Kevo. Environmental variables include photosynthetically active  
577 radiation (a-b, PAR), vapour pressure deficit (c-d, VPD) and rainfall (e, f).  
578 Environmental variables were measured at the ecosystem (black lines) and at the branch  
579 level (red lines). Mountain birch transpiration per unit leaf area (g-h,  $T_{leaf}$ ) and  
580 ecosystem evapotranspiration (i-j,  $ET_{eco}$ ) are also shown. Standard error is shown as  
581 shaded grey.

582 **Figure 3.** Sub-daily responses of ecosystem evapotranspiration ( $ET_{eco}$ ) and mountain  
583 birch transpiration per unit leaf area ( $T_{leaf}$ ) to PAR (panels a,c) and VPD (panels b,d),  
584 measured at the corresponding ecological scale (i.e. ‘branch’ for  $T_{leaf}$  and ‘eco’ for  
585  $ET_{eco}$ ) in Abisko (red) and Kevo (blue).

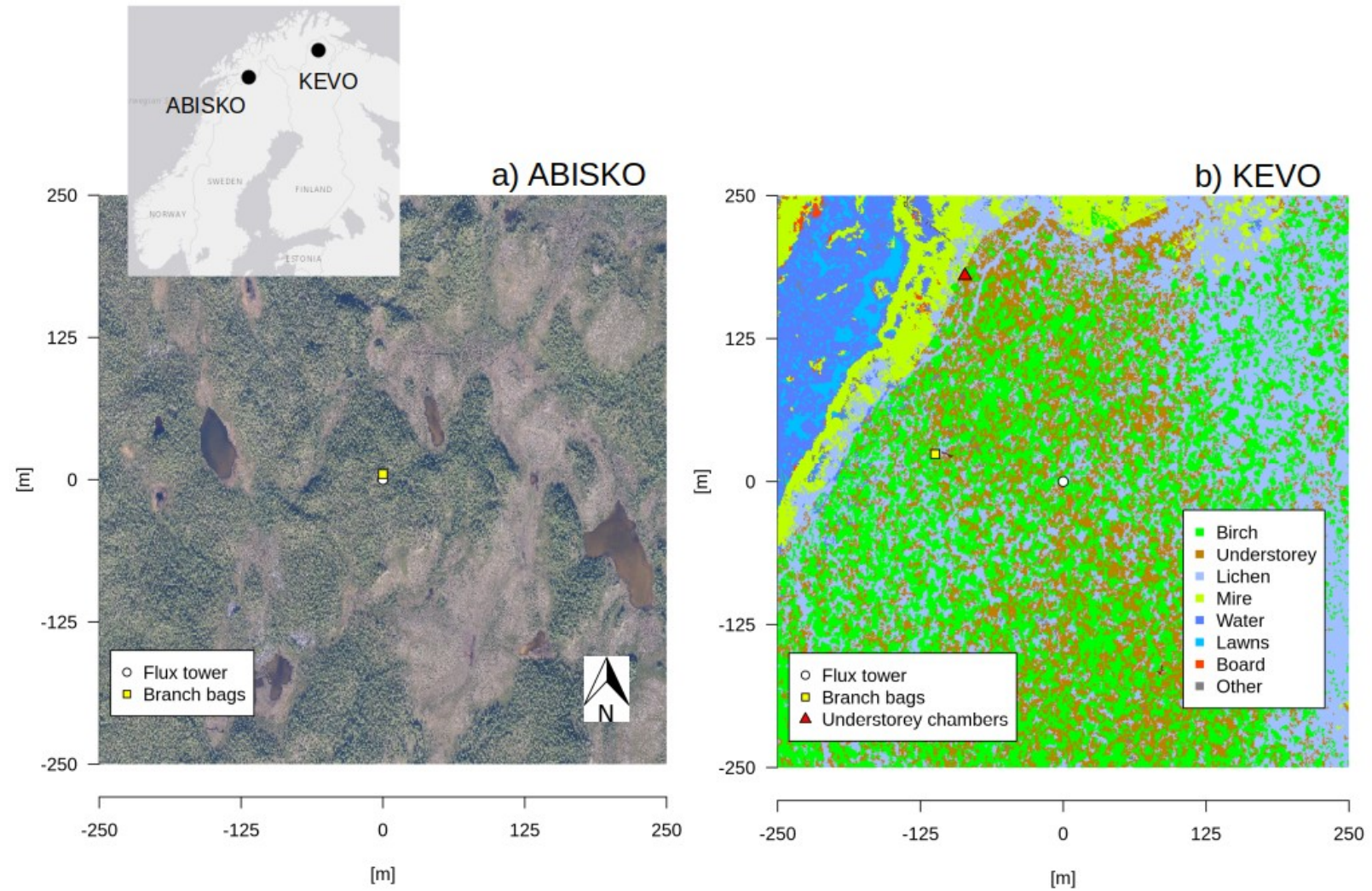
586 **Figure 4.** Response surfaces of modelled  $T_{leaf}$  (panels a, b) and  $ET_{eco}$  (panels c, d) as a  
587 function of VPD and PAR, in Abisko (panels a, c) and Kevo (panels b, d). Please note  
588 the different scales in the VPD axes in panels a and b compared to panels c and d.

589 **Figure 5.** Seasonal course of daily ecosystem evapotranspiration ( $ET_{eco}$ , black lines)  
590 and upscaled birch transpiration ( $T_{birch}$ , grey lines), for Abisko (a) and Kevo (b). The  
591 shaded regions in panels a and b depict upscaled  $T_{birch}$  using mean $\pm$ SE values of LAI  
592 (Table 1). Daily percentage of  $T_{birch}/ET_{eco}$  for Abisko (c) and Kevo (d). Panel (f) shows  
593 evapotranspiration components and their upscaled values for Kevo only:  $ET_{eco}$  (black  
594 line),  $T_{birch}$  (grey line),  $ET_{shrub}$  (purple line),  $ET_{lichen}$  (green line),  $ET_{upscaled}$  (asterisk).

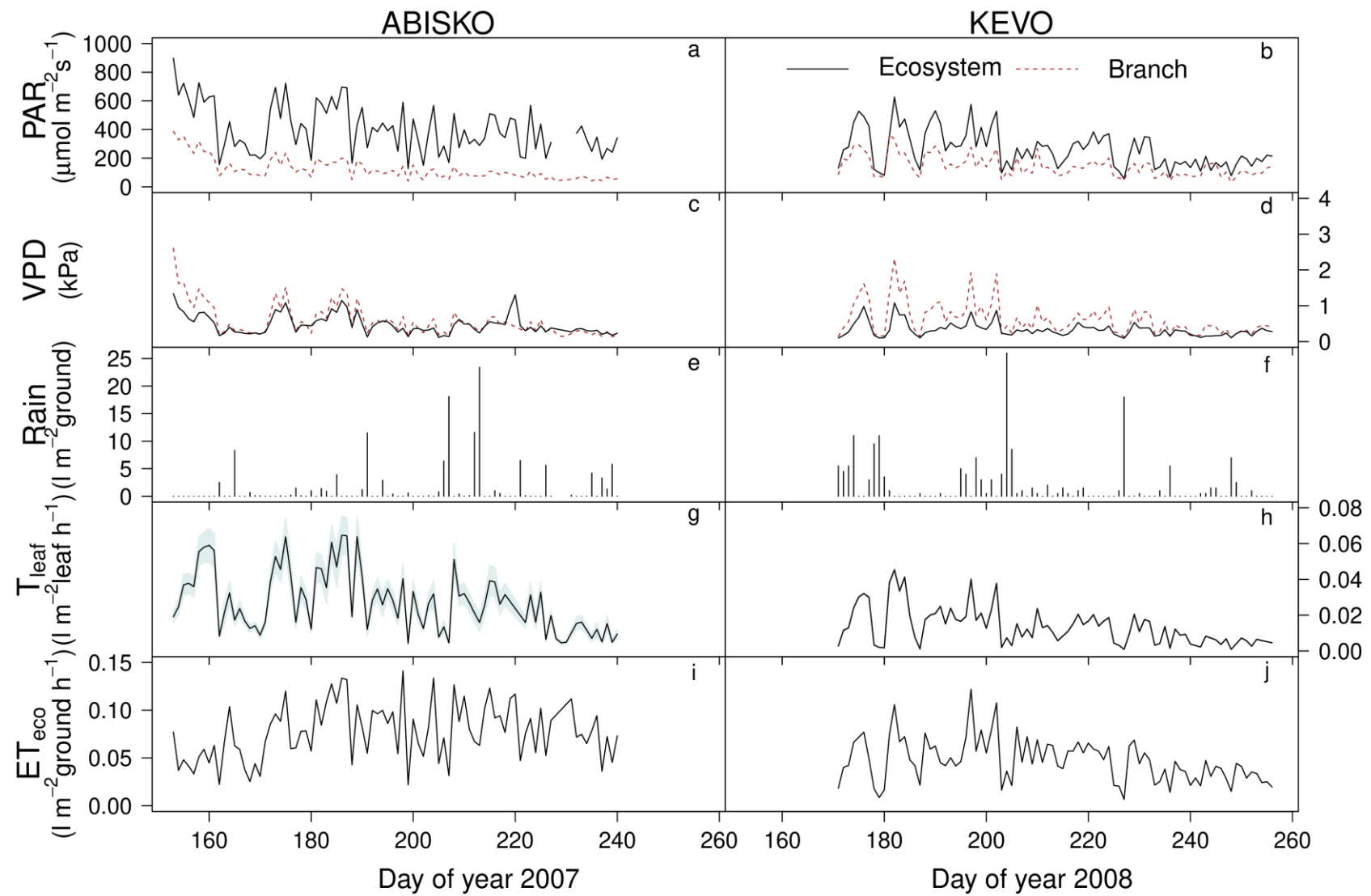
595 **Figure 6.** Variation of daily  $T_{birch} / ET_{eco}$  in response to  $VPD_{eco}$  (a),  $PAR_{eco}$  (b) and  
596 SMD (c), for Abisko (red) and Kevo (blue). Models summary are shown in Table S3.

597 Significant interaction between site and environmental value is shown in solid line and  
598 no-significant interaction in dashed line.



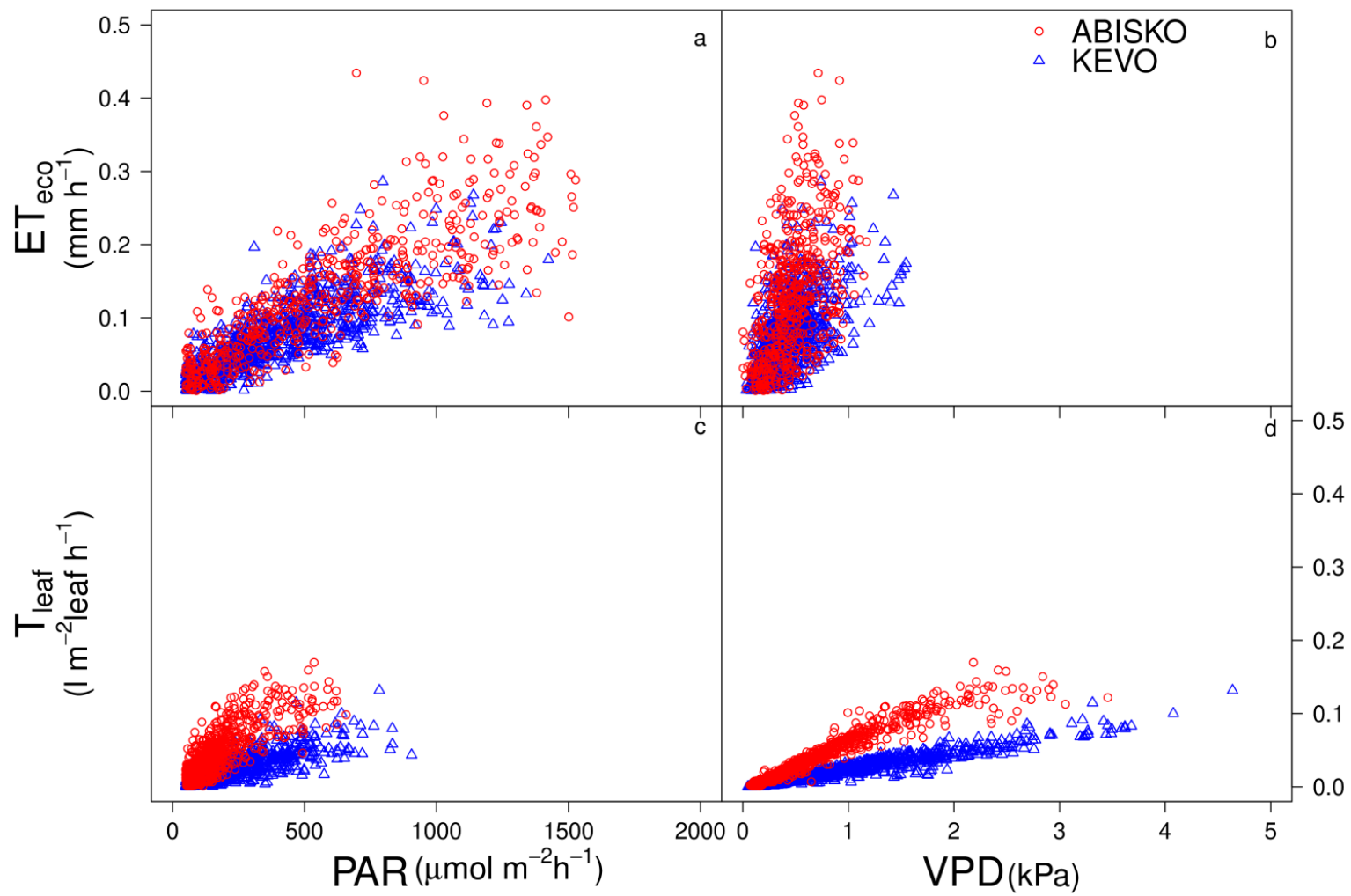


599 **Figure 1**

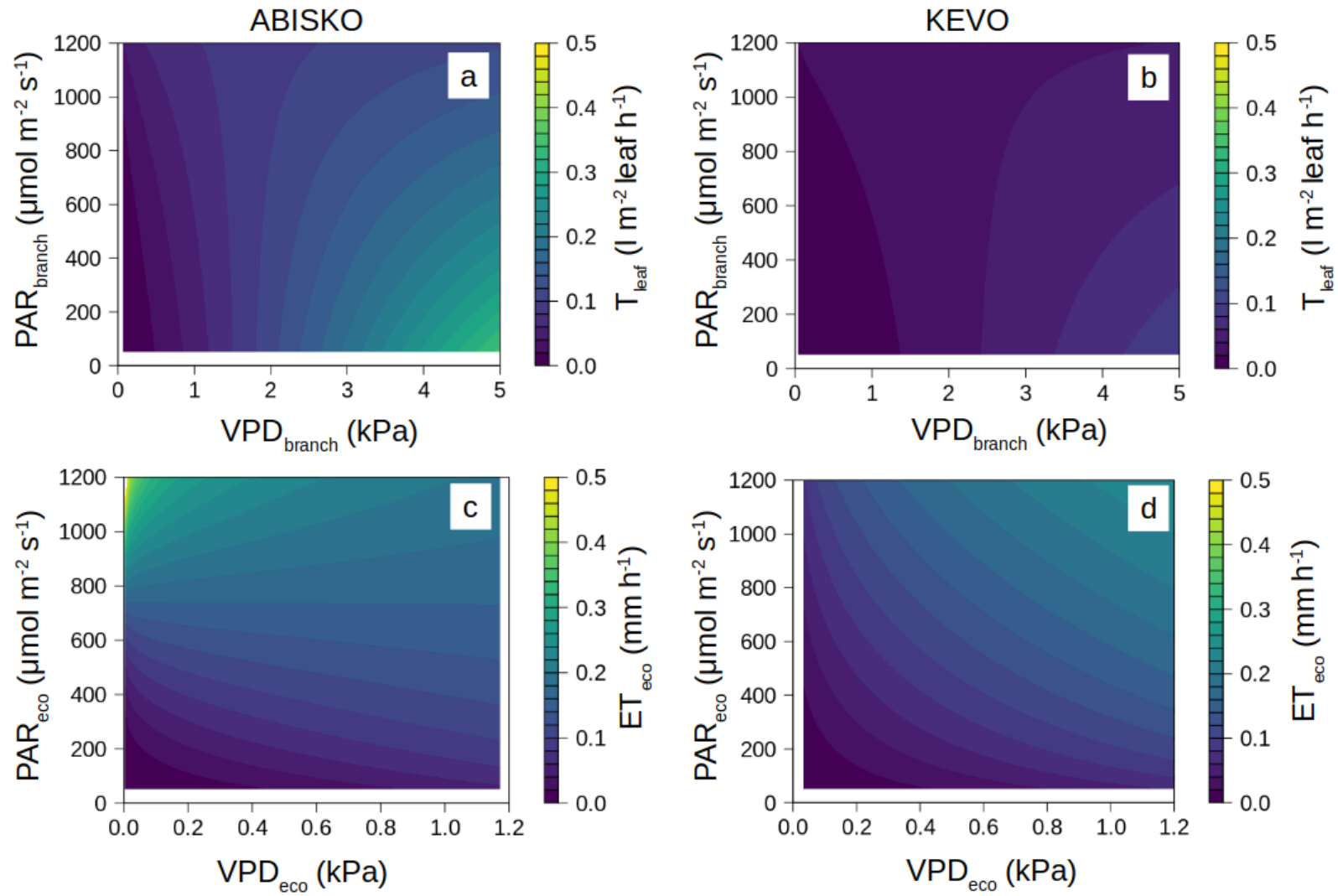


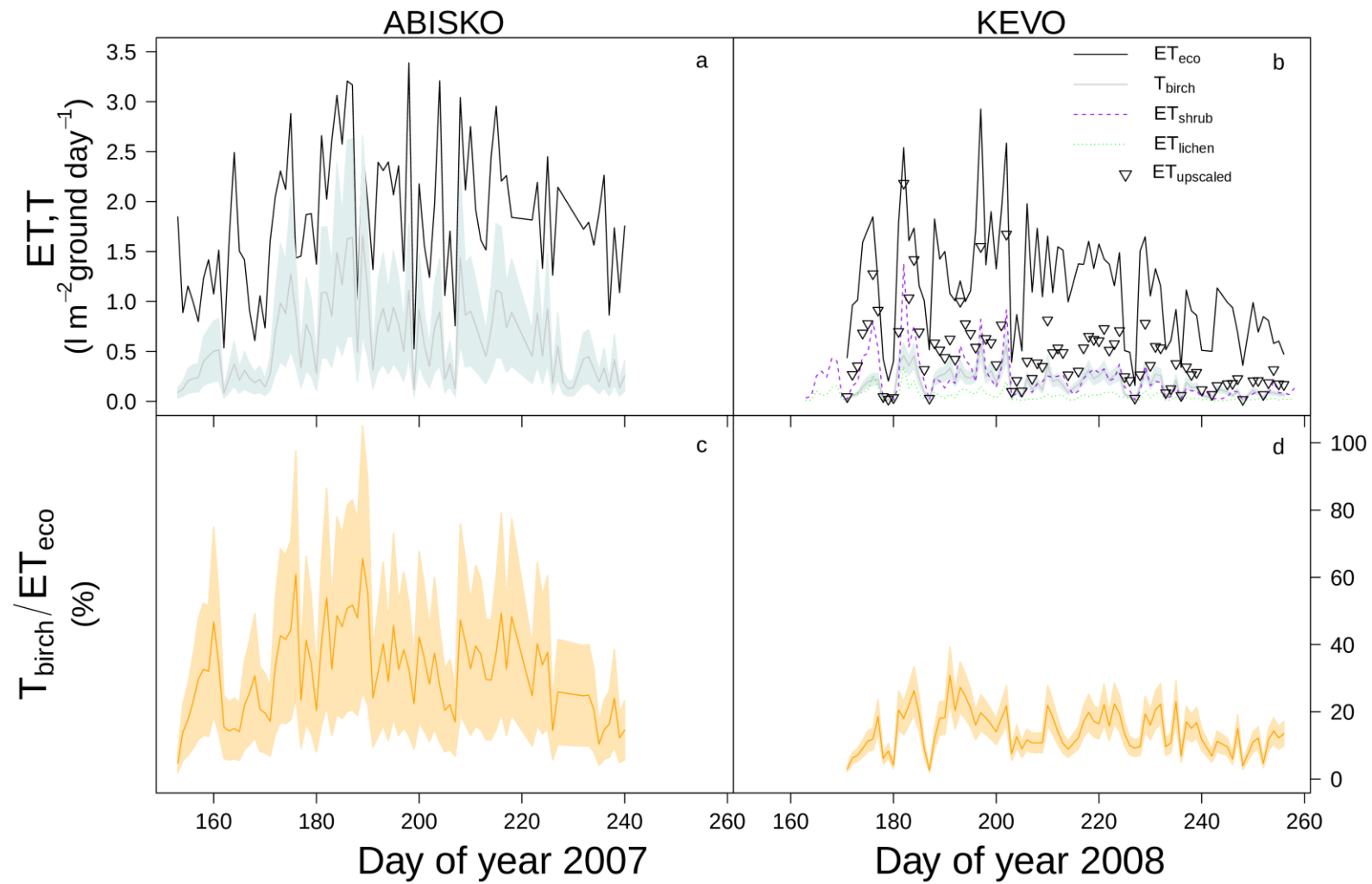
600  
601 **Figure 2**





603 **Figure**





605 **Figure 4.**

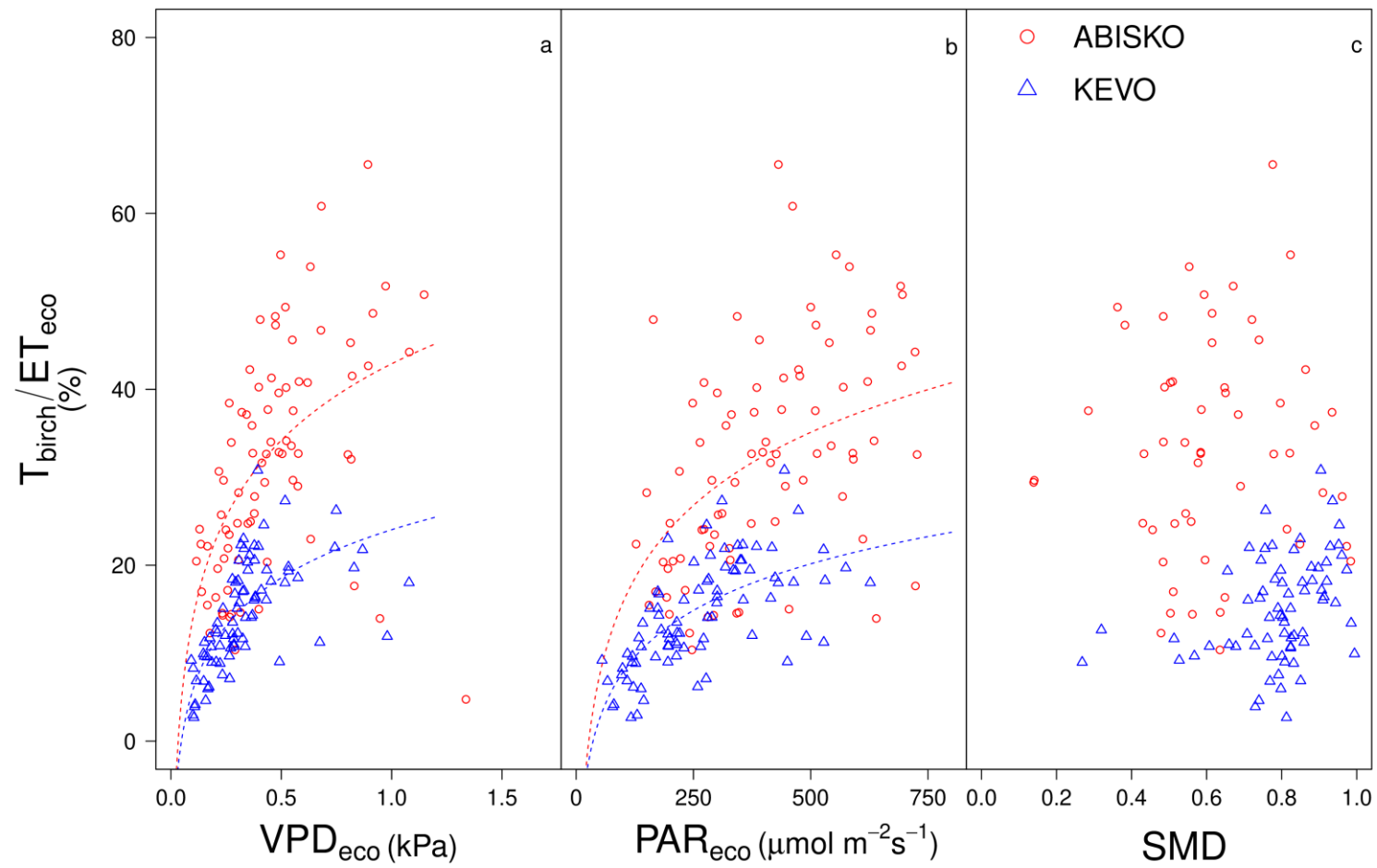
606

607

608 **Figure 5**

609

610



611  
612  
613  
614



615

616 **Figure 6**